Journal of Energy and Natural Resources
2022; 11(2): 52-59
http://www.sciencepublishinggroup.com/j/jenr
doi: 10.11648/j.jenr.20221102.14
ISSN: 2330-7366 (Print); ISSN: 2330-7404 (Online)

Flow Distortion Effects of a Three-Dimensional Ultrasonic Anemometer and Its Impact on Measurements

Jacob Oduogo*, Henry Barasa

Department of Physics, Masinde Muliro University of Science and Technology, Kakamega, Kenya

Email address:
joduogo@mmust.ac.ke (J. Oduogo), hbarasa@mmust.ac.ke (H. Barasa)
*Corresponding author

To cite this article:
Jacob Oduogo, Henry Barasa. Flow Distortion Effects of a Three-Dimensional Ultrasonic Anemometer and Its Impact on Measurements. *Journal of Energy and Natural Resources*. Vol. 11, No. 2, 2022, pp. 52-59. doi: 10.11648/j.jenr.20221102.14

Received: May 18, 2022; **Accepted**: June 15, 2022; **Published**: June 27, 2022

Abstract: The sonic anemometer is widely recognized as a precise and accurate instrument for measuring and studying atmospheric wind speed and turbulence that works on the principle of measuring the difference in the transit time of acoustic pulses along a known path length. Desirable characteristics of the sonic anemometer include lack of moving parts, linear dynamic response, and good directional response. However, the sensor probes and support structures inevitably lead to a deformation of the flow field being examined resulting in transducer shadowing and flow distortion errors. An empirical method of determining the effects of flow distortion errors on measurements is utilized. While deviations in the horizontal wind are negligible, investigations clearly indicate the need for correction of raw data on vertical wind measurements. Simulations have been conducted using a synthetic time series to determine the impact of observed errors on turbulence, with indications that measurements have a dependence on the angle of attack. Using the series at angles of elevation varying between -12° and 12°, a deviation in turbulence by over 30% is observed for certain wind directions. Matrices derived from the errors at different angles of attack have been used to correct standard ten-minute time series of field data resulting in a decrease in the measured turbulence strength by between 7 and 10%.

Keywords: Flow Deformation, Atmospheric Boundary Layer, Wind Direction, Wind Elevation, Turbulence Strength

1. Introduction

A precise knowledge of wind characteristics at a prospective site is essential for successful planning and implementation of wind energy projects. In many applications such as wind resource assessment, power performance testing and characterization of acoustic emission, it is the mean speed (usually averaged over 10 minutes) at a certain height above ground that is of interest. The cup anemometer is undoubtedly the most widely used instrument in meteorological and wind power applications and remains to date the most popular wind speed sensor [1]. However, for detailed analysis, wind measurements need to be made using more accurate and precise instruments. One of the major shortcomings of the cup anemometer is its inertia and dynamic filtering effects whose sequel is overestimation of the mean wind speed, often referred to as 'over-speeding' and underestimation of the spectral power in the wind [2]. This inability of the cup anemometer to follow wind speed fluctuations is a problem that has been known for decades and has led to the development of models that describe its characteristics [3]. The other shortcomings of the cup anemometer are its non-cosine response to vertical wind, frictional effects in the bearing caused by changes in weather and climatic conditions, and its inability to measure wind direction [4]. While a cup anemometer lacks directional information, the ultrasonic anemometer includes wind speed magnitude and direction. However, the sensor probes and support structures inevitably lead to a deformation of the flow field being examined [5]. Transducer shadowing is a well-known effect in sonic anemometry that causes attenuation of the mean wind component along the sensor axis by formation of a turbulent wake behind the transducer [6] the transducers and support structures also cause flow disturbances under certain orientations leading to deflection and distortion of the wind vector [7]. To minimize transducer

shadowing in anemometers with orthogonal transducer geometry, a linear relationship was assumed between velocity attenuation along the transducer path length and the angle between flow and path length [6]. Non orthogonal anemometers eliminated shadowing altogether by shifting all transducers from the horizontal plane into the vertical non orthogonal geometry which made them no longer independent [8]. Estimations of flow distortion effects have been done using potential flow theory by researchers such as [9-11], though theoretical methods remain restricted because there is no limit to the complexity of structure of flow around probes. Thus, studying flow deformation within controlled conditions and adapting their performance to situations in the atmospheric boundary layer remains a plausible option in mitigating flow distortion errors.

The atmospheric boundary layer (ABL) is defined as the vertical extent above the earth's surface where shear stress is variable and the wind structure is influenced by surface friction, temperature gradient and the rotation of the earth. Within this layer is the atmospheric surface layer (ASL) which is the lower 10% of the ABL where the flow is not affected by the earth's rotation and is therefore characterized by an approximately constant shear stress [12]. Strong vertical gradients controlling the transfer of momentum, moisture and heat exist in this region. Using the Monin-Obukhov similarity theory, the vertical behavior of dimensionless mean flow and turbulence properties can be described by atmospheric parameters such as gradients, variances and covariances which when normalized by the appropriate powers of the scaling velocity and scaling temperature become universal functions of the ratio of the height above the surface of the earth to a scaling length (Obukhov length). Turbulent transport in the atmosphere can therefore be expressed by the fluxes of momentum, heat, and moisture in terms of their gradients in the vertical direction. The momentum flux, also referred to as the Reynolds shear stress is defined as the mean product of the velocity fluctuations.

$$\tau = \rho\overline{u'w'} \tag{1}$$

Where ρ is the density of air and u' and w' are respectively the horizontal and vertical velocity fluctuations.

Accurate measurements in the ABL can therefore be largely useful in complementing theoretical studies in atmospheric science as well as providing new insights into the energy balance closure problem.

2. Operation Principle of the Instrument

The sonic anemometer works on the principle of measuring the time it takes an ultra-high frequency acoustic pulse (typically 100 kHz) to traverse a known path length in the direction of the wind and opposed to it. If transit time difference Δt is measured simultaneously in air velocity U, the relationship between this time difference is [13]:

$$\Delta t = \frac{2d}{a^2}U \tag{2}$$

where a is the speed of sound and d, the path length. The speed of sound in air can be calculated using the equation:

$$a^2 = \gamma RT(1 + 0.51q) \tag{3}$$

where γ is the ratio of specific heats, R the gas constant and q the specific humidity.

Equation (3) shows that the speed of sound depends on temperature and consequently the measurement of windspeed in sonic anemometers that employ this relation will depend on changes in ambient temperature. This relationship is utilized by the sonic anemometer in the measurement of temperature. Contemporary sonic anemometers employ run-time method to sequentially determine velocities along the sound paths between transducers [14]. Non-orthogonal three-dimensional (3-D) sonic anemometers have three transducer pairs aligned facing each other and oriented at an angle to the horizontal flow as shown in figure 1.

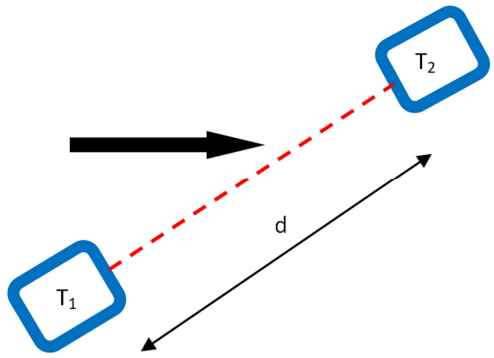

Figure 1. *Sketch of a transducer pair showing the acoustic path between two transducers* T_1 *and* T_2 *and the distance* d *between them.*

The time of flight of the acoustic wave travelling from the emitting transducer T_1 to the receiving transducer T_2 is measured when it is oriented with the flow (t_1) and when it is against it (t_2). Assuming a uniform flow field, the apparent speed of the "downwind" sound pulses is given by:

$$\frac{d}{t_1} = a.cos\alpha + U_d \tag{4}$$

while the apparent speed of the "upwind" sound pulses is given by:

$$\frac{d}{t_2} = a.cos\alpha - U_d \tag{5}$$

where U_d is the speed of flow along the sound path and α is defined as:

$$\alpha = \arcsin\left(\frac{U_n}{a}\right) \tag{6}$$

U_n being the speed of flow normal to the sound path. The speed of flow of fluid is then given by:

$$U_d = \frac{d}{2}\left(\frac{1}{t_1} - \frac{1}{t_2}\right) \tag{7}$$

Given the path length, the speed of wind can be measured

using the transit times only. This is the technique used by the commercial Thies 3-D sonic anemometer (shown in figure 2) used in this investigation. The three measurement paths of the anemometer are perpendicular in relation to each other with the transducer pairs facing each other functioning both as acoustic transmitters and receivers.

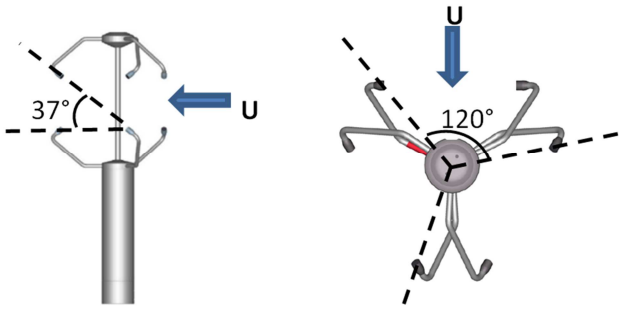

Figure 2. *Side and aerial view sketches of the Thies 3-D ultrasonic anemometer. The transducer pairs are oriented at* 120^0 *azimuth intervals at an inclination of* 37^0 *from the horizontal.*

The mean values are worked out sequentially from six individual measurements along the paths and the time required to complete one measurement cycle is approximately $3.5mS$ at 20°C with the maximum measuring speed $(75m/s)$ [15]. This measurement time is only limited by the velocity of sound over the measurement path and determination of wind speed is in principle independent of atmospheric factors such as temperature and humidity.

3. Method

Investigations of the ultrasonic anemometer were performed in the acoustic wind tunnel of the University of Oldenburg. This acoustic wind tunnel is a closed loop (recirculation type) wind tunnel with a high homogeneity and uniformity of flow. The flow of the wind tunnel differs across the stream by less than 0.2% and the background turbulence is about 0.3% at 50m/s. Experiments were done in the open test section of the tunnel with dimensions 0.8m x 1.0m x 1.8m (height x width x length) and sets of built-in pressure holes and pitot tubes in combination with a setra 239 piezoelectric pressure transducer used as reference wind speed sensors.

3.1. Experiments

The anemometer was assessed for horizontal wind speed and direction measurements by setting it vertically on a turntable positioned at the nozzle of the wind tunnel. To generate different flow directions the turntable was systematically rotated in steps of 2° azimuth angles up to 360° by a stepper motor controlled via LabView software. Non-horizontal wind measurements were performed by elevating the anemometer at 3°, 6°, 12° and 24° using a manual tilting mechanism and then rotating it in 2° azimuth steps as in the measurements with the upright anemometer. Figure 3 shows photographs of the setup for a non-horizontal measurement regime for three azimuth angles with the anemometer elevated at 12°.

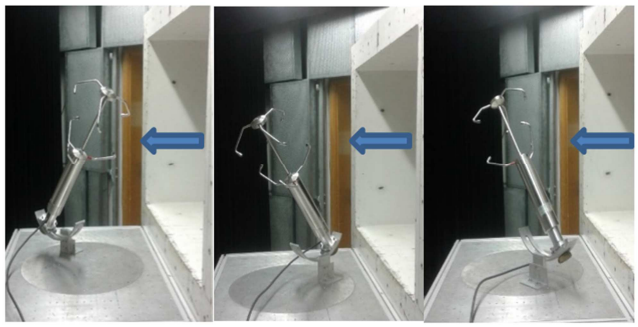

Figure 3. *Photograph of anemometer setup for investigating response to vertical wind at three different angles of attack.*

All measurements were conducted with set reference wind speeds within the range of $0m/s$ to $16m/s$. The signal connections from the dynamic, static and barometric pressure sensors, temperature sensor, humidity sensor and the anemometer were made via NI 6211 DAQ to a measuring PC with LabVIEW software. Data was then simultaneously acquired at a sampling rate of $100\,KHz$ for $20s$ with a waiting time of $10s$ between wind speed intervals to ensure flow stability. Field data was collected on five consecutive days for a continous period of five hours daily at a sampling rate of $50\,KHz$.

3.2. Simulations

The sonic anemometer has a non-orthogonal probe head, therefore, to simulate the measurements by the sonic anemometer, the main wind vector is decomposed to components along the sensor paths using the geometry and orientation of the anemometer. These non-orthogonal velocity components are then transformed into the required cartesian coordinate system. Figure 4 shows an aerial view of the anemometer, the z axis points upwards and is perpendicular to the x-y plane.

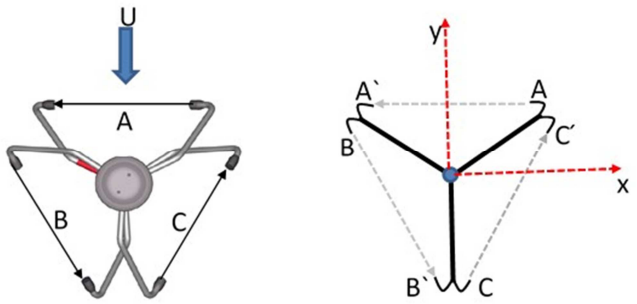

Figure 4. *Sketches of the probe viewed from above showing the acoustic paths of the three sensors and* x *and* y *axes of cartesian coordinates.*

When mounted in the atmosphere, the y axis points to the north direction. Using geometrical considerations of the sensor positions, the unit vectors along the sonic paths AA´, BB´ and CC´ are expressed as:

$$t_1 = cosA_v cosA_h\, x + cosA_v sinA_h\, y + sinA_v\, z \qquad (8)$$

$$t_2 = -cosB_v cosB_h\, x - cosB_v cosB_h\, y + sinB_v\, z \quad (9)$$

$$t_3 = -cosC_v cosC_h\, x + cosC_v cosC_h\, y + sinC_v\, z \quad (10)$$

Where h and v are the horizontal and vertical components along the sensor paths while $x\, y$ and z are unit vectors in cartesian coordinates.

The wind vector is expressed in cartesian coordinates as $U = U_x\, x + U_y\, y + U_z\, z$ and the projection of the wind vector on to the acoustic paths is $S = U.t$. The transformation matrix derived from these relations was used in converting the wind vector along the acoustic paths to cartesian coordinates and vice versa.

4. Results and Discussion

The sonic anemometer used in these investigations is a three-dimensional device and to determine the response to wind direction, three selected wind speeds of $7m/s$, $11ms$, $15m/s$ have been measured with varying wind direction by changing the azimuth angle between 0° and 360°. Figure 5 shows the plots of the directional response for the three speeds. Through normalization with the reference wind speed, it is observed that the horizontal speeds almost perfectly follow the reference speed with deviations not exceeding the specified accuracy for this anemometer (2%) [15].

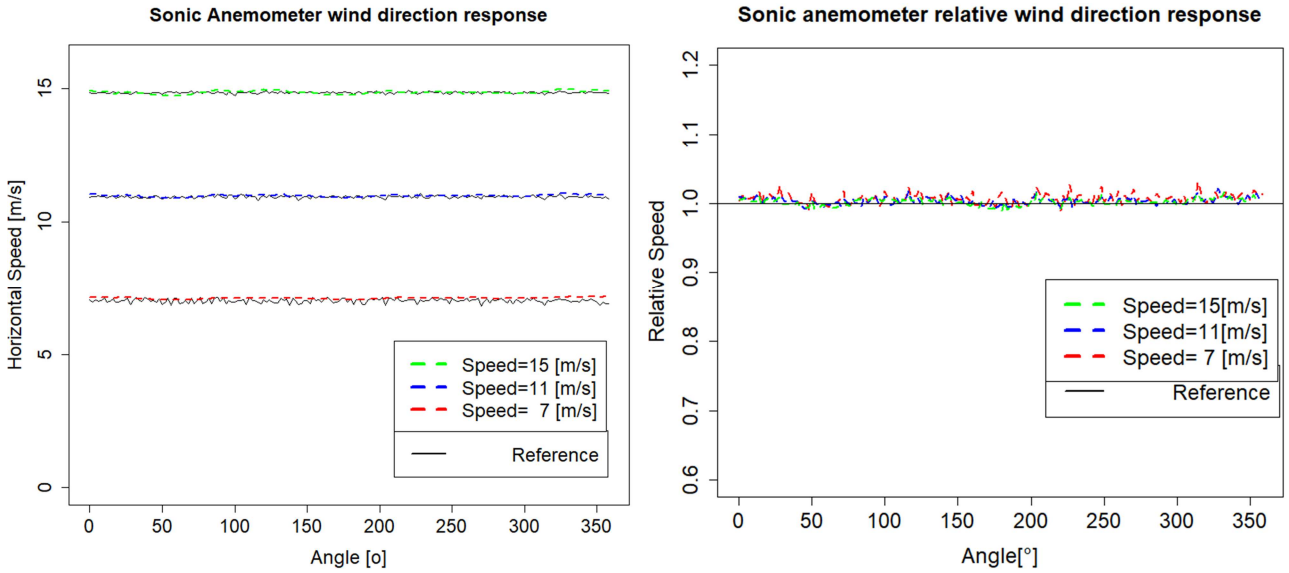

Figure 5. *Horizontal wind speed measurements for three selected wind speeds with varying wind direction. The reference wind speeds are shown as continuous lines.*

The vertical component of wind however is seen to vary with the reference speed even with the upright anemometer. Figure 6 shows plots of the variations in the vertical wind with direction.

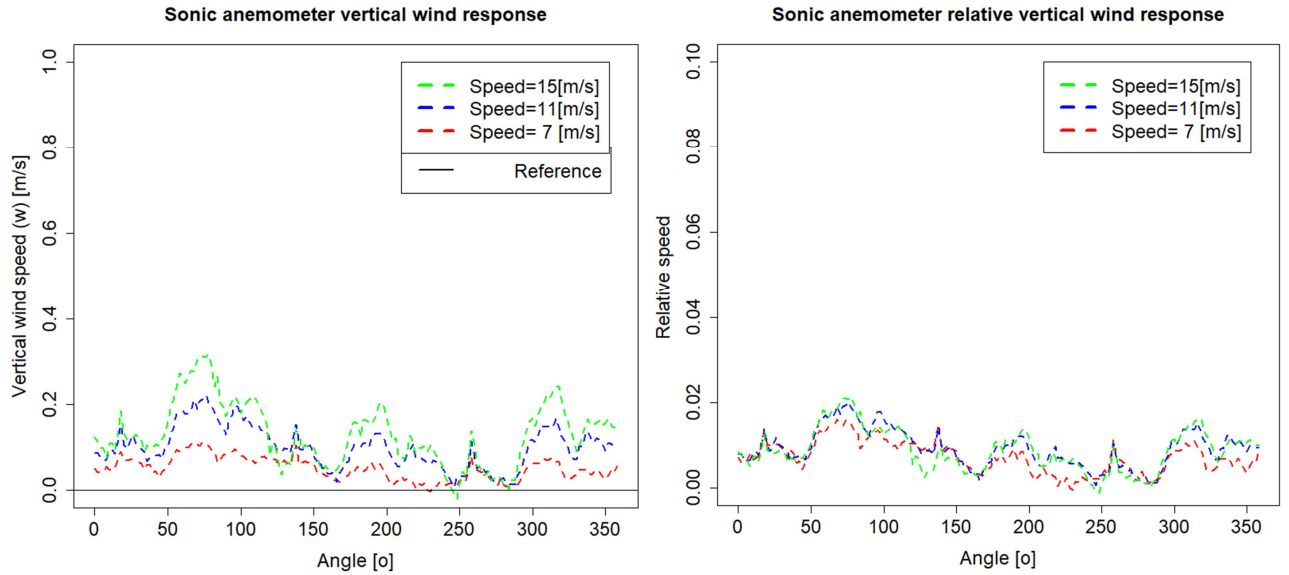

Figure 6. *Vertical wind speed and relative measurements for three selected wind speeds with varying wind direction.*

The anemometer is observed to have a positive offset of the vertical component that varies with wind speed and the

deviation is observed to exceed 2% of the reference value of the main flow speed in some directions even though this component should be negligible for the upright anemometer. This clearly indicates the need for correction of raw data for vertical wind measurements. A normalization of the vertical component to the reference value indicates a linear influence of wind speed (see figure 6). To establish the relationship between the main flow speed and this component, the sonic speed is plotted against the reference wind speed with the anemometer at fixed azimuth positions and varying wind elevations. Figure 7 shows plots of the vertical wind speed and deviations against reference wind speed at an azimuth angle of 0°.

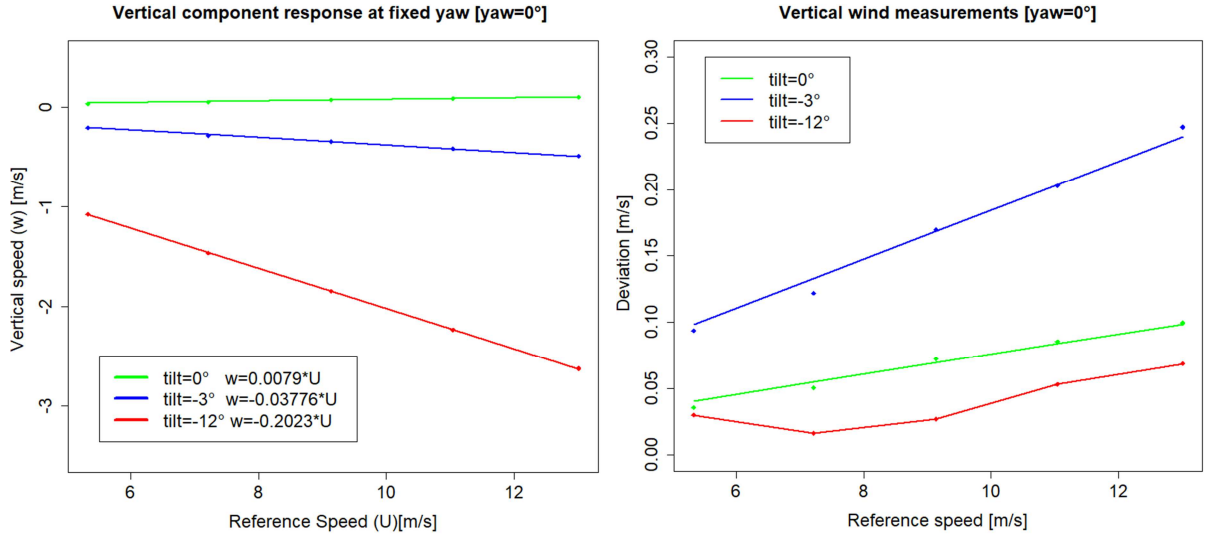

Figure 7. *Vertical wind and deviations versus the reference measurements at three different angles of elevation.*

While the general relationship between vertical component and the reference speed is linear, deviations in the measurements exhibit near linear while others non-linear behavior (See figure 7). The deviations due to flow distortion can therefore be said to show non-linear behavior with varying speed. Based on these measurements, an estimated characteristic of the vertical component that is dependent on the main flow speed and angle of elevation is derived as in equation (11).

$$w = k * \theta * U + M_c \tag{11}$$

Where θ is the angle of elevation, Mc the observed deviation and k a constant.

To validate the model, equation (11) was used to generate simulated vertical wind speeds at different directions and elevations. Figure 8 shows deviations from the reference value of simulations and measurements at 0° azimuth and elevation of -12° and -6°.

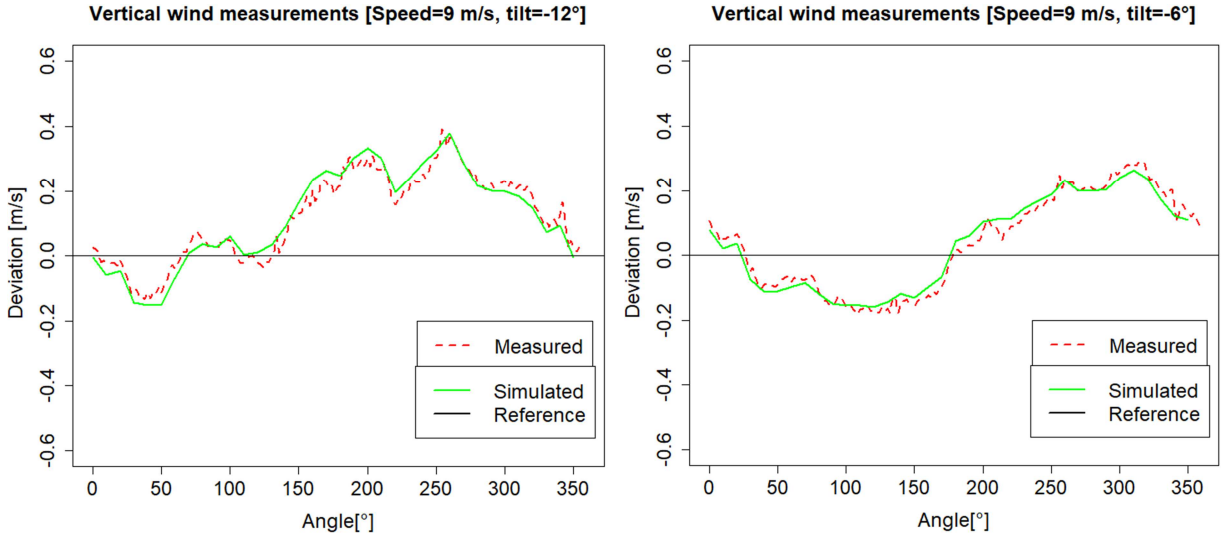

Figure 8. *Deviations in the measured and simulated vertical wind measurements for two different elevations at a selected speed of* $9m/s$.

The effect of these systematic deviations caused by flow distortion on the statistical values of the measurements was then determined by using a synthetic stochastic time series. This series with a mean of $9m/s$ was generated and applied to the simulation model for selected mean wind directions of flow and a table of statistical values produced. Figure 9 is the original

time series and the measured time series for a mean wind direction of 0° at two selected angles of elevation (-6° and 6°). The plots show a wider difference between the measured and actual values for the negative elevation angle and a smaller deviation for the positive angle. A probable reason for this difference is that in the case of the negative elevation, the probe head faces the flow and may result in a greater distortion of the wind within the measurement volume of the sensors while for the positive elevation the wind first passes through the sensors before being further distorted by the probe head.

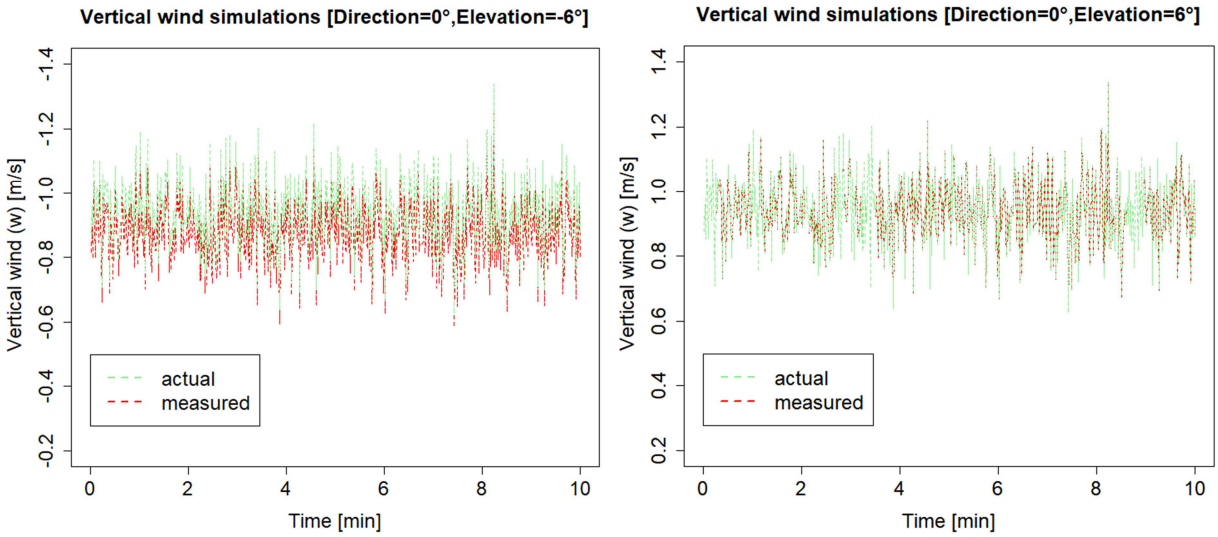

Figure 9. *Time series of the original and the measured values at a wind direction of 0°.*

The stochastic time series is used in the calculation of the actual and measured mean and turbulence values for different wind directions and elevations. The calculations are done in six wind direction sectors with six elevations covering both upwind and downwind.

The calculated statistical values show dependence on the angle of attack. Transducer induced flow distortion affect wind speed variance through amplification, attenuation, and crosstalk. Though the combination of the three sensors of the anemometer and their supports are expected to distort the flow in a complex way, attenuations are observed to occur under certain orientations of the probe with amplifications occurring when two sensors are aligned with the main free stream. This observation suggests that the measurement volume is more affected by the wakes of the transducers when they are aligned with the flow which is anticipated because more wakes form on the measurement path of the transducer pairs if they are in alignment with the direction of wind. The wind elevation and speed dynamics were examined by calculating wind data in 5° and $1m/s$ bin intervals respectively for vertical wind and main flow speed measurements. Figure 10 shows Histograms of a selected standard ten-minute time series for wind elevation and speed at a mean wind direction of 11°.

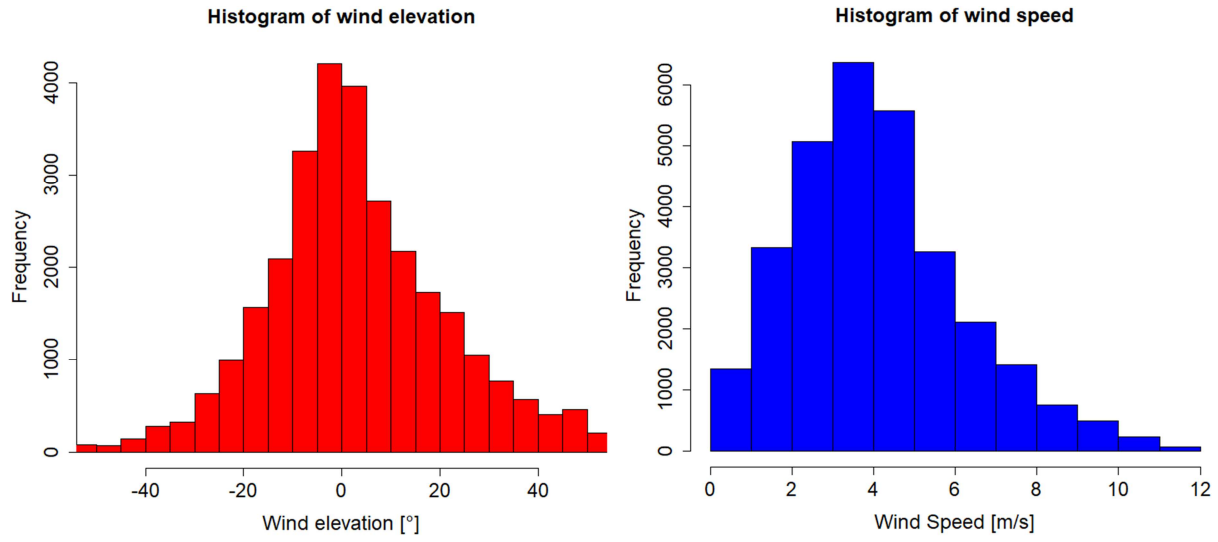

Figure 10. *Histograms of wind elevation and speed at a mean wind direction of 11°.*

While the histogram of the ten-minute series of speed follows the characteristic Weibull distribution with a range of $12m/s$, that of the elevation covers a range of angles with majority counts falling within the scope of the investigated

angles (±15°) and reduced counts at higher and lower end of the bins. The error in the vertical wind is estimated using matrices derived from observed deviations at different directions, elevations, and wind speeds. To apply the correction, the wind direction and elevation were calculated from measured horizontal and vertical wind components and the observed vertical deviation that corresponds most closely with the investigated orientations of the wind vector looked up from the correction matrices and subtracted from the measurements. The impact of the error on the measurements was then determined by comparison of statistical quantities calculated from ten-minute time series of the measured wind.

Figure 11 are plots of the measured and corrected ten-minute time series of the vertical component and a zoom of the time series displaying a one-minute series drawn from the first minute of the series.

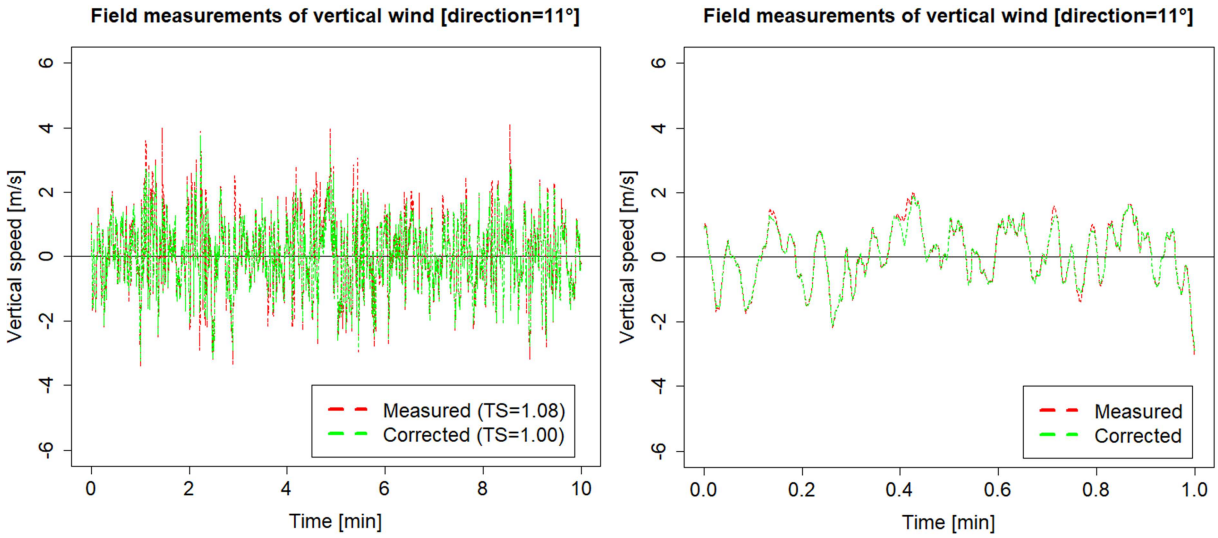

Figure 11. *Ten- minute time series of measured vertical wind and one-minute time series drawn from the first minute of the series.*

The ten-minute time series shown in figure 11 falls within the first sector of the investigated wind directions, the results indicate that the uncorrected vertical component overestimates the turbulence strength by about 8%. The correction was applied to such series of a daily five-hour field data collected for five consecutive days covering two wind direction sectors. The performance such non-orthogonal sonic anemometers has been the subject of much discussion in recent years following findings that they underestimated vertical winds and heat fluxes by 10-15%. Efforts have been made to understand the contribution of errors introduced in field measurements to the energy balance equations and broadly to the energy balance closure problem [16]. Previously, comparisons of turbulence data from hundreds of monitoring stations led to conclusions that the errors were a consequence of the tilted geometry and non-orthogonal design [17]. Currently, flow distortion by the probes of sonic anemometers is touted as the main source of error in commercial designs [18].

5. Conclusion

The three-dimensional ultrasonic anemometer was investigated to determine the effects of flow distortion on measurements under controlled conditions of flow. Even though the effects of sensor-induced flow distortion on the horizontal component were found to be negligible, the deviations of the vertical wind measurements were significant. A model is developed that is dependent on the azimuth angle, elevation angle and wind speed. Simulations performed using a synthetic time series are used to determine the impact of the errors on statistical measurements. The calculated statistical values show a significant dependence on the angle of attack with higher deviations for directions in which the measurement volume is in the wake of two transducers aligned with the flow. Measurements are improved by subtraction of the observed deviations and the impact on statistical values derived from the standard ten-minute time series. Analysis of field data collected for five hours daily for five consecutive days with wind directions covering two 60°-sectors indicate significant changes in the measured vertical fluctuations due to flow distortion, resulting in an increase of about 9% in the turbulence strength. Since wakes behind transducers and supporting struts of a sonic probe will most likely behave differently under steady and turbulent conditions, the employed settings are not exactly transferable to atmospheric measurements making further investigations to examine flow under turbulent conditions necessary for further improvement of the field measurements.

Acknowledgements

The authors gracefully thank the following institutions: German Academic exchange service for the Scholarship (ST32-91609111 for Jacob Oduogo), The center for wind energy research of the University of Oldenburg for the facilities, kind support and hospitality and Masinde Muliro

University for granting Jacob Oduogo permission to be away from the University.

References

[1] P. Santiago, C. Javier and S. Felix, "The cup anemometer, the fundamental instrument for the wind energy industry", *Sensors,* pp. 21418-21482, 2014.

[2] L. Kristensen und O. Hansen, "Distance constant of the Riso cup anemometer", *Riso National Labotatory, Technical Report* R-1320, 2002.

[3] J. C. Wyngaard, "Cup, Propellor Van and Sonic Anemometers in Turbulence", *Annual Review Fliud Mechanics,* pp. 13: 399-423, 1981.

[4] S. Pindado, A. Sanz und A. Wery, "Deviation of cup and anemomoter calibration results with frequency", *Energies 5,* pp. 683-701, 2012.

[5] C. Kraan und W. A. Oost, "A new way of anemometer calibration and its application to asonic anemometer", *Journal of Atmospheric Oceanic technologies,* Bd. 6, pp. 516-524, 1989.

[6] J. Kaimal, J. Gaynor, H. Zimmerman und G. Zimmerman, "Minimizing flow distortion errors in sonic anemometer", *Boundary layer Meteorology 53 (1),* pp. 103-115, 1990.

[7] E. Vidal und Y. Yee, "Data colection of high resolution 3-D sonic anemometer measurements", *American meteorological society,* pp. 1-5, 2003.

[8] S. F. Zhang, J. C. Wyngaard, J. A. Businger und S. P. Oncley, "Response characteristics of the sonic anemometer", *Journal of Atmospheric and Oceanic Technology,* Bd. 3, pp. 315-323, 1986.

[9] A. J. Dyer, "Flow distortionby supporting structures", *Boundary layer meteorology,* Bd. 20, pp. 243-251, 1981.

[10] J. C. Wyngaard, "The effect of probe induced flow distortion on atmospheric turbulence measurements", *Journal of applied meteorology,* Bd. 20, pp. 784-794, 1981.

[11] H. G. Norment, "Calculation of Wygaard distortion coefficints and turbulence ratios and influence of instrument induced wakes on accuracy", *Journal of atmospheric and oceanic technology,* Bd. 9, pp. 505-519, 1992.

[12] J. C. Kaimal und F. J. J, *Atmospheric boundary layer flows*, New York: Oxford Uninersity Press, 2004.

[13] B. Perdesen, T. Perdesen, H. Klug, N. Borg, N. Kelley und J. Dahlberg, "Recomemned practices on wind turbine testing", *Research and development on wind energy conversion systems*, Glasgow, 2003.

[14] R. C. Baker, Flow Measurement Handbook: Industrial Designs, Operating Principles, Perfomance and Applications, *Cambridge University Press*, 2000.

[15] T. G. Adolf, Thies Ultrasonic anemometer operating instructions, Göttingen, Germany: ThiesClima, 2014.

[16] P. Li and Wang, A Nonequilibruim Thermodynamic Approach to Surface Energy Balance Closure, *Geophysical Research Letters*, Volume 47 issue 3, 2019.

[17] J. M. Frank, W. Massman and B. E. Ewers, Underestimation of Heat flux due to vertical velocity errors in sonic anemometers, *Agricultural and Forestry Meteorology*, 171: 72-81, 2013.

[18] J. Kochendorfer, J. Meyers, J. Frank, W. J. Massman, W. J., and M. W. Heuer. 'How well can we measure vertical wind speed: Implications of fluxes of energy and mass'. *Boundary Layer Meteolrology* 53-103, 2014.